A 2-AXIS GYROSCOPE WITH A SYNCHRONOUSLY-DRIVEN DUAL MASS

T. Akashi, H. Funabashi, Y. Omura, M. Fujiyoshi, Y. Hata, and Y. Nonomura
Toyota Central R&D Labs., Inc., Nagakute, Aichi, JAPAN

ABSTRACT

We report a detuned 2-axis yaw-and-roll gyroscope with a single sensor element. We designed and fabricated a novel structure composed of a synchronously driven dual mass and three types of supporting beams to limit the movable direction of each mass. The designed resonant frequencies agreed well with the measured values, which resulted in 2-axis detuning ratios of -0.7 and -2.2%. The fabricated gyroscope showed a cross-axis sensitivity of +/-2.7%. The test results demonstrated that the gyroscope simultaneously detects yaw and roll rates with low cross-axis sensitivity.

KEYWORDS

Gyroscope, yaw, roll, dual mass, cross-axis sensitivity.

INTRODUCTION

MEMS inertial sensors have been used to support safety in driving a vehicle. In particular, a perpendicular-axis MEMS gyroscope for yaw-rate detection is applied to vehicle-stability control to prevent skidding. Such a perpendicular-axis gyroscope has been reported to improve its performance [1-2].

In contrast, a lateral-axis gyroscope for roll-rate detection is not frequently reported [3]. This seems to be partly because the perpendicular-axis gyroscope is applicable to a roll-rate sensor by changing its mounting direction. For a conventional automotive application, the lateral-axis gyro can be used as a rollover sensor to prevent accidents.

We predict that in the future, next-generation vehicles will need to monitor their body motion more precisely in order to realize an automated driving or advanced driving-safety system. As such, the advanced vehicle control system will need to sense bank angle and slow spin. Therefore, the sensor applied to the system must be able to detect yaw and roll rates with high resolution, high reliability, and long-term stability. Moreover, the sensor should be compact and inexpensive because at least two sensors are required in order to realize a fail-safe system in automobiles. One way to solve this problem is to detect the 2-axis yaw-and-roll rate with only one sensor element.

However, only a few multi-axis gyroscopes with a single sensor element have been reported [4-5]. W.K. Sung et al. reported the hollow-disk pitch-and-roll resonant gyroscope. Their gyroscope exhibited relatively large cross-axis sensitivity of 20%. We consider that for a 2-axis gyroscope with lower cross-axis sensitivity, the movable direction of a Coriolis mass should be controlled, and the mass should vibrate in translational direction as precisely as possible.

In the present paper, we report a detuned 2-axis yaw-and-roll gyroscope with a dual mass, which vibrates synchronously in translational direction.

SENSOR STRUCTURE AND WORKING PRINCIPLE

Figure 1 illustrates the sensor-element structure of the proposed 2-axis gyroscope. The gyroscope structure is three-dimensionally formed on both 15-μm-thick top and 150-μm-thick bottom Si layers of an SOI substrate. The sensor-element has two Coriolis masses composed of the bottom-layer frame masses 1 and 2. Masses 1 and 2 are connected to the bottom-layer connecting plate via the top-layer outer Z-beams and bottom-layer Y-beams, respectively. The connecting plate is supported by the bottom-layer folded X-beams and has drive and monitor combs. Since the connecting plate is mechanically connected to the two masses, the drive comb vibrates the two masses synchronously. Therefore, there are no phase differences between the two masses.

Inner frame mass 1 is connected to the structurally differential zigzag-shaped Z-electrode (ZSZ) [6] via the bottom-layer linkage X-beams. The ZSZ capacitively detects the Z-directional displacement corresponding to the applied roll rate. The ZSZ is supported by the inner Z-beams. On the other hand, outer frame mass 2 is mechanically and electrically connected to the top-layer Y-electrodes that capacitively detect the Y-directional displacement corresponding to the applied yaw rate.

Mass 1 is movable in the X and Z directions, whereas mass 2 is movable in the X and Y directions. The movable direction of each mass is limited by the separated multi-beam structure composed of the three types of supporting beams.

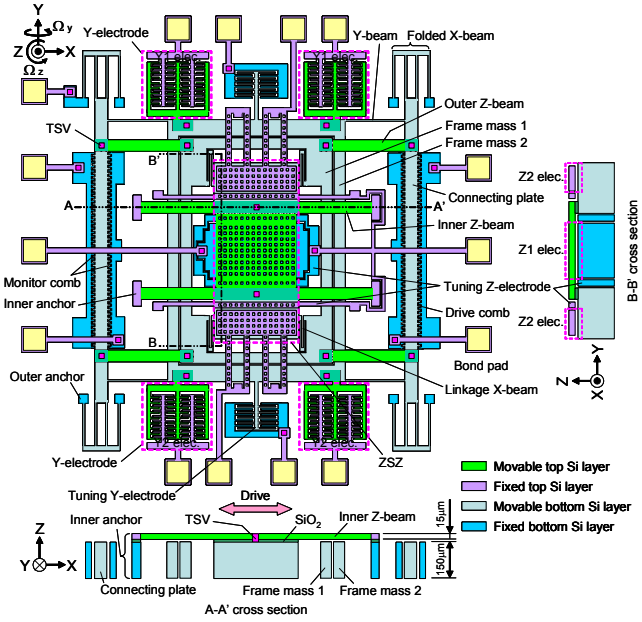

Figure 1: Sensor-element structure of the proposed 2-axis gyroscope for detecting yaw and roll rates.

The proposed yaw-and-roll gyroscope works as follows. Regarding the yaw-rate detection, when yaw rate Ωz is applied, mass 2 moves in the Y direction, whereas mass 1 moves only slightly in the Y direction due to the high Y-directional stiffness of the Z-beams. Then, the Y-electrodes on mass 2 differentially detect the capacitive changes corresponding to the applied yaw rate. In contrast, regarding the roll-rate detection, when roll rate Ωy is applied, mass 1 moves in the Z direction, whereas mass 2 moves only slightly in the Z direction due to the high Z-directional stiffness of the bottom-layer Y-beams. Then, the parallel-plate ZSZ mechanically connected to mass 1 moves in the Z direction and capacitively detects the roll rate.

The gyroscope detects each rate with each electrode connecting each of the Coriolis masses. Since the movable direction of each mass is restricted by the separated beams, this sensor-element structure can maintain the cross-axis sensitivity to be as low as possible.

DESIGN

We designed the 2-axis gyroscope as a detuned gyroscope because high stability and robustness is required for an automotive application. Table 1 shows one of the designed values of the gyroscope. The designed frequency range was set to be less than 10 kHz.

An FEM simulation using ANSYS™ software was implemented to design the 2-axis detuning ratio. Figure 2 shows the FEM-simulated modal analytical results. The first mode was designed to be the drive mode. In this mode, the two frame masses were synchronously driven in the X direction, whereas the decoupled ZSZ was not driven in the X direction. The second and third modes were designed to be the sense modes for yaw and roll rates, respectively. In the second yaw-rate sense mode, mass 2 with the Y-electrodes was driven in the Y direction, whereas mass 1 did not move. In the third roll-rate sense mode, mass 1 and the ZSZ mechanically connected to mass 1 was synchronously driven in the Z direction, whereas mass 2 with the Y-electrodes did not move in the Z direction.

Accordingly, mass 1 moves only in the X and Z directions, whereas mass 2 moves only in the X and Y directions. Each of the masses is considered to have two degrees of freedom. Thus, each of the masses is mechanically decoupled to sense each Coriolis force induced by the 2-axis angular rates. The simulated results supported the above-mentioned working principle.

Table 1: Designed values of the 2-axis gyroscope.

	Design values
Drive-mode frequency	7567 Hz
Yaw sense-mode frequency	7586 Hz
Roll sense-mode frequency	7787 Hz
Detuning ratio for yaw sense mode	-0.25%
Detuning ratio for roll sense mode	-2.9%
Folded X-beam width	10.0 μm
Linkage X-beam width	6.0 μm
Y-beam width	11.0 μm
Z-beam width	110 μm

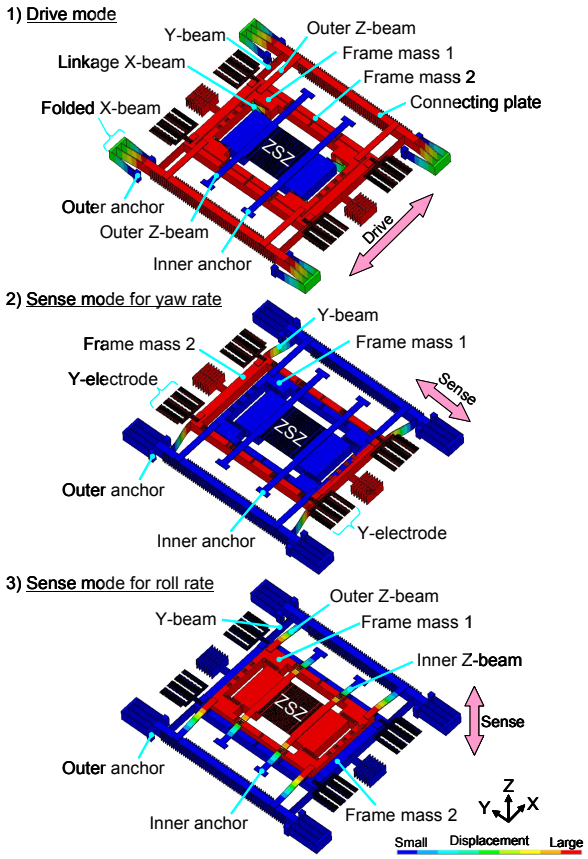

Figure 2: FEM modal analysis results of the proposed 2-axis gyroscope. Red structures undergo large displacement, whereas blue structures undergo small displacement.

FABRICATION

Figure 3 shows the fabrication process flow. We used an SOI wafer with a 15-μm-thick top Si layer, a 2-μm-thick buried oxide layer, and a 200-μm-thick bottom Si layer.

First, a poly-Si mushroom-shaped structure (pSiMS) was fabricated to prevent a movable structure from sticking Z-directionally (Step 1) [7]. Next, a poly-Si TSV was fabricated as follows. First, USG and poly-Si films were deposited, and the mask composed of their films was patterned. Then, a 5-μm-wide, 12-μm-long, and 15-μm-deep through-hole was fabricated by DRIE with the mask. Subsequently, the buried oxide layer was etched by RIE and BHF. In addition, the through-hole was refilled with doped poly-Si by LPCVD. After that, the doped poly-Si and poly-Si-mask films were etched back and the USG mask film was removed. Again, USG and doped poly-Si films were deposited and patterned (Step 2). After that, the remaining USG film was patterned for structuring the top Si layer. Subsequently, an Al-Si-Cu film was deposited and patterned (Step 3). Moreover, DRIE was implemented to form top-layer structures (Step 4). Next, the processed wafer was temporarily glued onto a 500-μm-thick support Si wafer. After that, the bottom Si layer was thinned down to a thickness of 150 μm (Step 5). A resist-mask pattern was then formed to structure the thinned bottom Si layer. DRIE was

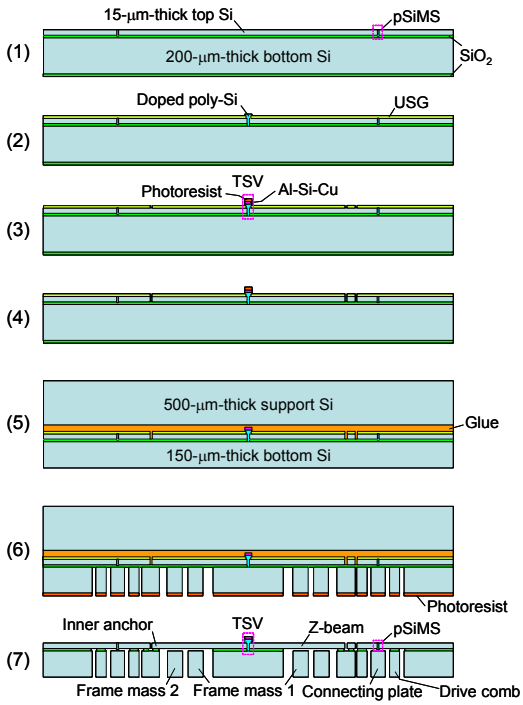

Figure 3: Fabrication process flow for the 2-axis gyroscope. Cross-sectional view of A-A' in Figure 1.

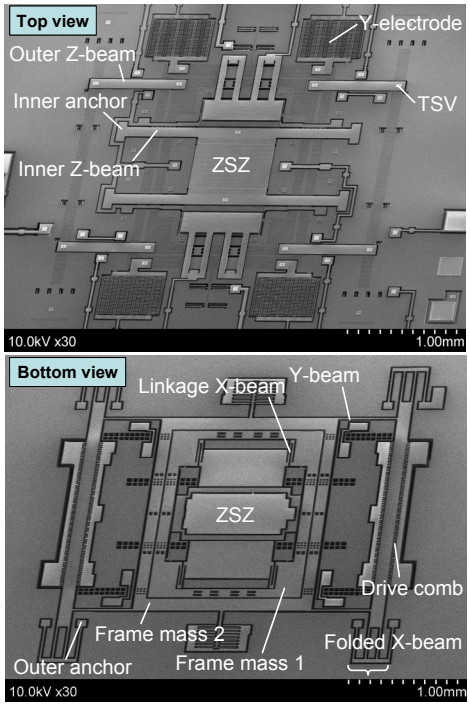

Figure 4: Top and bottom views of the 2-axis gyroscope.

implemented (Step 6). After DRIE of the bottom Si layer, the processed wafer was detached from the support Si wafer. Finally, the structure was released with HF vapor sacrificial etching (Step 7).

The 2-axis gyroscope was successfully fabricated using the above-mentioned process. Figure 4 shows SEM photographs of the fabricated 2-axis gyroscope.

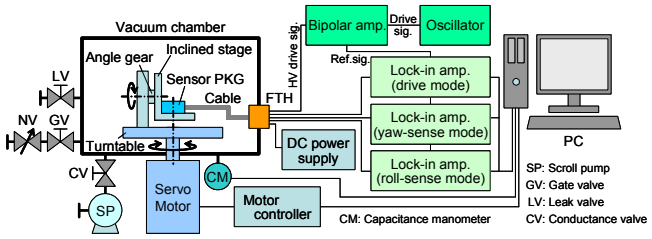

Figure 5: Test system for evaluating the 2-axis gyroscope.

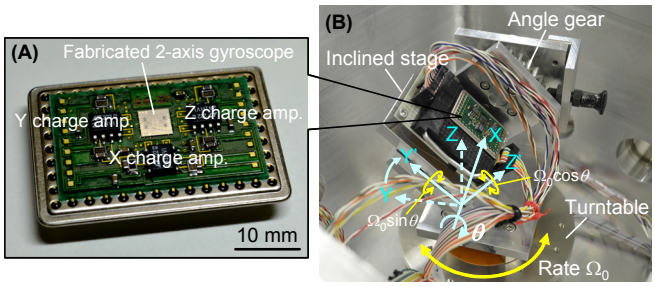

Figure 6: Experimental setup for 2-axis simultaneous measurement. (A) The fabricated gyro was mounted on a circuit board on an uncapped sensor-package. (B) The sensor-package was set on the inclined stage on the turntable in the vacuum chamber. Normally, the package was capped.

EXPERIMENTAL RESULTS

Experimental Setup

The fabricated 2-axis gyroscope was tested using an in-house vacuum chamber with a turntable. Figure 5 illustrates the test system for evaluating the gyroscope characteristics. The chamber pressure was manually controlled using a needle valve (NV). The pressure was precisely monitored by a ceramic capacitance manometer. The pressure was normally maintained at 100.0 Pa. The turntable in the vacuum chamber was rotated clockwise and counterclockwise by an AC servo motor placed outside the chamber. The full-scale rate range of Ω_0 was +/-180°/s. An angle gear can manually set an inclined stage at an angle in the range of 0 to 90°. The gyroscope characteristics were evaluated using three lock-in amplifiers.

Figure 6 shows the fabricated 2-axis gyroscope mounted to an uncapped sensor-package and a close-up of the experimental setup for 2-axis simultaneous measurement. The fabricated gyroscope was mounted on a circuit board with three charge amplifiers. When the turntable is rotated at rate Ω_0, the inclined stage provides the gyroscope with 2-axis angular rates simultaneously. This means that for stage angle θ, the angular rates of $\Omega_0 \sin\theta$ and $\Omega_0 \cos\theta$ are induced for the Y' and Z' axes, respectively. Thus, this mechanical system is simple for the 2-axis simultaneous measurement. In order to simultaneously measure 2-axis angular rates, the gyroscope was placed on the inclined stage on the turntable in the vacuum chamber, as shown in Figure 6 (B).

Sensor Characteristics

Table 2 shows the measured resonant frequencies in the drive and sense modes. The measured results agreed well with the designed values. However, small differences between

Table 2: 2-axis gyro resonant frequency characteristics.

	Measured values	Measured /Design ratio
Drive mode frequency	7565 Hz	100.0%
Yaw sense-mode frequency	7620 Hz	100.4%
Roll sense-mode frequency	7733 Hz	99.3%

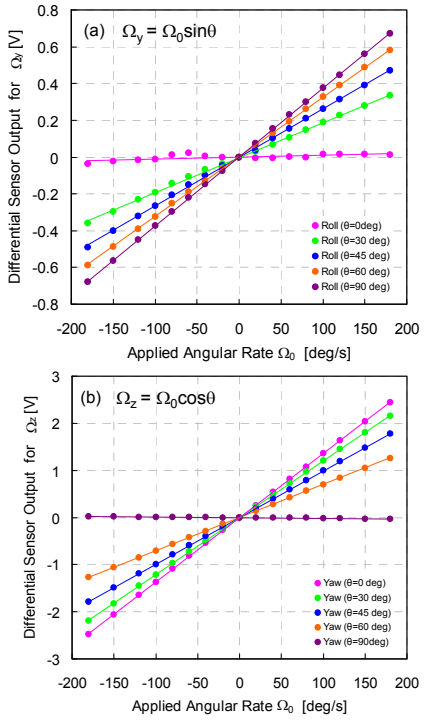

Figure 7: Measured 2-axis simultaneous sensor outputs. (a) Yaw-rate and (b) roll-rate detection (pressure: 100 Pa).

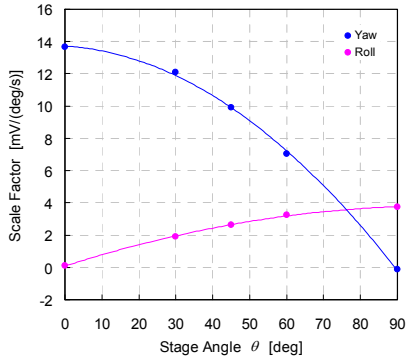

Figure 8: Measured yaw-and-roll scale factors as a function of stage angle (pressure: 100 Pa).

the design and measured resonant frequencies caused the relatively large change in the detuning ratio. The measured yaw and roll detuning ratios were -0.7 and -2.2%, respectively. The measured Q factors of Q_x, Q_y, and Q_z were 582, 794, and 690, respectively.

Figure 7 shows the measured 2-axis simultaneous sensor-outputs depending on the stage angle θ. The measured roll-rate scale factor was 3.75 mV/(°/s) at θ of 90°, while the measured yaw-rate scale factor was 13.7 mV/(°/s) at θ of 0°. When the yaw and roll rates were applied, the non-linearity was +/-0.4% and +/-2% (FS: +/-180°), respectively. The scale factors were changed according to θ, as shown in Figure 8. The yaw-and-roll sensitivity ratio was 3.65, which was induced due to the difference in the detuning ratio.

When the yaw and roll rates were applied, the measured cross-axis sensitivity was 2.7 and -1.0%, respectively. Their values were corresponding to 4.8 and -1.8°/s at Ω_0 of 180°/s. The fabricated gyroscope exhibited low cross-axis sensitivity. This is because the dual mass is not only driven synchronously but is also decoupled by each separated beam.

CONCLUSIONS

A detuned 2-axis yaw-and-roll gyroscope with a dual mass was presented. Each of the masses is synchronously driven and mechanically decoupled in each sense direction. The test results demonstrated that the fabricated gyroscope simultaneously detects yaw and roll rates with low cross-axis sensitivity.

REFERENCES

[1] U.M. Gómez, B. Kuhlmann, J. Classen, W. Bauer, C. Lang, M. Veith, E. Esch, J. Frey, F. Grabmaier, K. Offterdinger, T. Raab, H.J. Faisst, R. Willig, and R. Neul, "New Surface Micromachined Angular Rate Sensor for Vehicle Stabilizing Systems in Automotive Applications", in *Technical Digest of Transducers'05*, Seoul, Korea, 2005, pp. 184-187.

[2] Y. Mochida, Y. Kato, Y. Konaka, A. Mori, M. Kobayashi, and S. Kobayashi, "Precise MEMS Gyroscope with Ladder Structure", in *Technical Digest of Transducers'07*, Lyon, France, 2007, pp. 2529-2532.

[3] Z.Y. Guo, Z.C. Yang, L.T. Lin, Q.C. Zhao, J. Cui, X.Z. Chi, and G.Z. Yan, "A Lateral-Axis Micromachined Tuning Fork Gyroscope with Novel Driving and Sensing Combs", in *Technical Digest of Transducers'09*, Denver, CO, USA, 2009, pp. 288-291.

[4] S.R. Chiu, C.Y. Sue, C.H. Lin, S.T. Lin, S.C. Lin, Y.W. Hsu, and Y.K. Su, "Design, Fabrication and Performance Characterizations of an Integrated Dual-Axis Tuning Fork Gyroscope", in *Proceedings of IEEE Sensors 2012*, Taipei, Taiwan, 2012, pp. 1612-1615.

[5] W.K. Sung, M. Dalal, and F. Ayazi, "A Mode-Matched 0.9 MHz Single Proof-Mass Dual-Axis Gyroscope", in *Technical Digest of Transducers'11*, Beijing, China, 2011, pp. 2821-2824.

[6] M. Fujiyoshi, Y. Nonomura, H. Funabashi, Y. Omura, T. Akashi, and Y. Hata, "An SOI 3-Axis Accelerometer with a Zigzag-Shaped Z-Electrode for Differential Detection", in *Technical Digest of Transducers'11*, Beijing, China, 2011, pp. 1010-1013.

[7] T. Akashi, H. Funabashi, and Y. Nonomura, "A Mushroom-Shaped Convex Poly-Si Structure for Preventing Z-Directional Stiction of an SOI-MEMS Device", in *Proceedings of MEMS 2011*, Cancun Mexico, 2001, pp. 201-204.

CONTACT

*T. Akashi, tel: +81-561-717171; t-akashi@mosk.tytlabs.co.jp